

Light curves and $H\alpha$ luminosities as indicators of ^{56}Ni mass in type IIP supernovae

A. Elmhamdi¹, N.N. Chugai², and I.J. Danziger³

¹ SISSA / ISAS , via Beirut 4 - 34014 Trieste - Italy

² Institute of Astronomy RAS, Pyatnitskaya 48, 109017 Moscow, Russia

³ Osservatorio Astronomico di Trieste, Via G.B.Tiepolo 11 - I-34131 Trieste - Italy

Abstract. The possibility is investigated that the $H\alpha$ luminosity at the nebular epoch may be an additional indicator of ^{56}Ni mass in type II supernovae with plateau (SNe IIP), on the basis of available photometry and spectra. We first derive the ^{56}Ni mass from the M_V magnitude on the radioactive tail using a standard approach. A confirmation of the correlation between ^{56}Ni mass and plateau M_V magnitude found recently by Hamuy (2003) is evident. There is strong evidence of a correlation between steepness of the V light curve slope at the inflection time and the ^{56}Ni mass. If confirmed, this relation may provide distance and extinction independent estimates of the amount of ^{56}Ni in SNe IIP. We then apply upgraded radioactive models of $H\alpha$ luminosity at the nebular epoch and claim that it may be a good indicator of ^{56}Ni , if mass, energy and mixing properties vary moderately (within factor ~ 1.4) among SNe IIP. This method of the ^{56}Ni mass determination from $H\alpha$ luminosities yields results which are consistent with the photometric mass of ^{56}Ni mass to within 20%. This result also implies that the parameters of SNe IIP events (mass, energy and mixing properties) are rather similar among the majority of SNe IIP, except for rare cases of SN II intermediate between IIP and IIL (linear), of which SN 1970G is an example.

Key words. (Stars:) supernovae: type IIP; Nucleosynthesis, abundances; Photometry, spectra.

1. Introduction

Supernovae type II with a plateau in the light curve (SNe IIP) are thought to be a spectroscopically and photometrically homogeneous family of core collapse supernovae (Filippenko 2001). The light curve of SN IIP is characterized by two distinct phases; a plateau with a duration of 60 – 100 days and a quasi-exponential tail at the later epochs. The plateau corresponds to the radiative cooling of the hot opaque envelope originally heated by the explosion (Grassberg et al. 1971). Variations of observational properties at the plateau phase are interpreted in terms of variation of ejecta mass, explosion energy, and radius of the progenitor (Litvinova & Nadyozhin 1985). The exponential tail is attributed to the instant reprocessing of the energy of radioactive decay of ^{56}Co (Weaver & Woosley 1980) and the luminosity at this stage is directly determined by the mass of ejected ^{56}Ni , a fact successfully exploited for SN 1987A (Catchpole et al. 1988).

The SN IIP phenomena are believed to originate from the explosion of red supergiant stars whose main sequence masses lie in the range 10 – 25 M_{\odot} ; precise boundary

are still a subject of controversy, as well as the mechanism(s) of explosion. The study of optical properties of SNe IIP provides a means of recovering their major characteristics (mass, energy, ^{56}Ni mass, asymmetry) and eventually to impose constraints on the explosion models and pre-supernova parameters. The ^{56}Ni mass is one of the crucial parameters since it presumably depends on the presupernova structure and the explosion model (Aufderheide et al. 1991) and can be directly measured.

The straightforward way to measure ^{56}Ni mass in SNe IIP is based upon the physical argument that the early (120–300 d) bolometric luminosity on the radioactive tail should be equal to the luminosity of radioactive decay of ^{56}Co . This is because at this stage the loss of the internal energy to expansion (pdV work) is small, while the envelope is nearly opaque to gamma-rays. This method was successfully used for SN 1987A (Catchpole et al. 1988; Bouchet & Danziger 1993) with estimates 0.08 M_{\odot} and 0.07 M_{\odot} , accordingly, and an average 0.075 M_{\odot} . The application of this method to other SNe IIP is, however, hampered by the lack of infrared observations longward of the I band. Note, the $UBVRI$ data account for about half of the luminosity at this age according to results for SN 1987A (Catchpole et al. 1988;

Schmidt et al. 1993). Therefore, for SNe IIP one uses the absolute flux in one band (e.g. V) or several bands in the optical, which, on being compared with the absolute flux of SN 1987A provides an estimate of ^{56}Ni mass. This method essentially assumes that the absolute flux in one or several optical bands is a constant fraction of the bolometric flux, i.e. the spectral energy distribution (SED) during the radioactive tail epoch is similar for all SNe IIP. Using this approach, Phillips et al. (1990) claimed that similar B and V absolute magnitudes of SN 1987A, SN 1969L and SN 1983K on the radioactive tail implies similarity of their ejected ^{56}Ni masses. A similar conclusion was made by Patat et al. (1994) from a study of a large sample of type II SNe. Schmidt et al. (1993) slightly modified this method applying a procedure of reconstruction of the light curve using a bolometric correction determined from SN 1987A data. Using a constant bolometric correction does not necessarily improve the accuracy of the determination of ^{56}Ni mass compared with the use of absolute magnitudes in one or several filters. Recently Hamuy (2003) using this method recovered ^{56}Ni mass for an extensive sample of SNe IIP and pointed to an interesting correlation of ^{56}Ni mass with the luminosity (M_V) on the plateau.

Here we revisit the problem of ^{56}Ni mass in SNe IIP, pursuing two major goals. First, we independently determine the ^{56}Ni mass for a different sample using a unified approach to distance determination and present a new correlation between ^{56}Ni mass and light curve shape. The second major goal is to check the possibility of the use of $\text{H}\alpha$ luminosity as a tracer of ^{56}Ni mass. This possibility is intriguing bearing in mind that in the case of high redshift SN IIP ($z \geq 0.05$) we face a problem of contribution of the host galaxy background, which will inhibit the confident estimation of the broad band magnitude at the radioactive tail phase. On the other hand, $\text{H}\alpha$ is not affected by the stellar background and thus may be used as an indicator of the ejected amount of ^{56}Ni . Nevertheless incorrect subtraction of any underlying H II region emission could hamper accuracy; identification of this narrow component in the blend would remove this problem. The use of $\text{H}\alpha$ as an indicator of ^{56}Ni mass is prompted by early radioactive models which show an expected proportionality between $\text{H}\alpha$ luminosity and the amount of ^{56}Ni (Chugai 1990). This has also been noted in connection with the comparison of light curve and $\text{H}\alpha$ luminosities for SN 1999em and SN 1987A (Elmhamdi et al. 2003).

The paper is organized as follows. We first select a sample of well observed SNe IIP with late photometry and spectra, and adopt appropriate distances and extinction (Sect. 2). We then apply the V light curve technique to estimate the ^{56}Ni mass for these supernovae and study correlations between the ^{56}Ni mass and light curve shape (Sect. 3). Then we use the late $\text{H}\alpha$ luminosity to derive ^{56}Ni mass (Sect. 4). Both photometric and spectroscopic ^{56}Ni mass are then compared and the implications are discussed (Sect. 5).

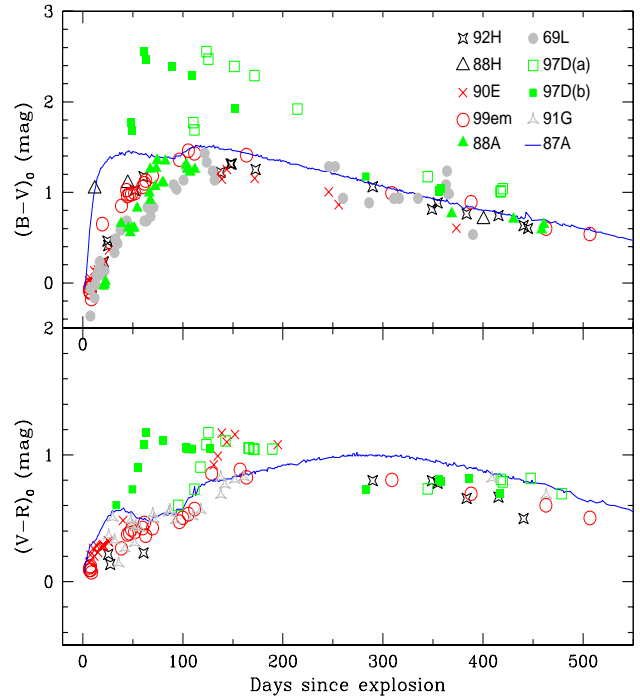


Fig. 1. The $B - V$ (upper panel) and $V - R$ (lower panel) intrinsic colour evolution of the SNe sample. Both options for SN 1997D are shown (sect. 4.2). The used reddening is reported in Table 1 (fourth column).

2. Sample, distance, extinction

Our basic sample consists of 9 SNe IIP, namely: SN 1987A, SN 1969L, SN 1988A, SN 1988H, SN 1990E, SN 1991G, SN 1992H, SN 1997D and SN 1999em, although throughout the paper we will be invoking other objects (SN 1970G, SN 1995ad, SN 1995V, SN 1995W, SN 1999gi and SN 1999eu). The events are selected on the basis of published and unpublished photometric and spectroscopic observations at the plateau and later epochs. The sample parameters are presented in Table 1 together with the corresponding references to the literature from which the photometry has been taken. In what follows we adopt the standard reddening laws of Cardelli et al. (1989). For the problem of ^{56}Ni determination the total extinction and distance estimates are of principal importance. Galactic extinction is removed using the map of galactic dust extinction by Schlegel et al (1998). The host galaxy reddening is then estimated from the $B - V$ and $V - R$ colour excess compared to the intrinsic colour curves of SN 1987A. This approach is justified by the fact that at the late photospheric phase SNe IIP seem to follow colour evolution similar to SN 1987A (Schmidt et al. 1992). The use of the $B - V$ colour alone to estimate the host galaxy reddening may present some problems, as in most cases it provides negative reddening. This point was noted also by Hamuy (2003) who used the $V - I$ index for an independent estimate of extinction.

Table 1. Parameters data of the SNe IIP sample

SN name	Parent galaxy	Distance (Mpc)	A_V^{tot}	M_V late slope mag (100d) $^{-1}$	References
1987A	LMC	0.05	0.6	0.976	1, 2
1999em	NGC 1637	8.8	0.31	0.97	3, 4, 5
1969L	NGC 1058	9.057	0.203	0.97	6, 7
1988A	NGC 4579	22.95	0.136	1.12	8, 9
1988H	NGC 5878	28.47	0.47	---	9
1990E	NGC 1035	16.18	1.2	0.86	11, 14
1991G	NGC 4088	14.11	0.065	1.11	10
1992H	NGC 5377	29.07	0.054	0.97	15
1997D	NGC 1536	16.84	0.07	0.87	12, 13, 16
1970G	NGC 5457	7.2	0.4	1.04	6, 17
1999gi	NGC 3184	10.91	0.65	---	18
1999eu	NGC 1097	---	---	---	19

REF:

1- Arnett 1996; 2- Hirata et al. 1987; 3- Baron et al. 2000; 4- Elmhamdi et al. 2003;

5- Hamuy et al. 2001; 6- Kirshner & Kwan 1975; 7- Patat et al. 1994; 8- Ruiz-lapuenta et al. 1990;

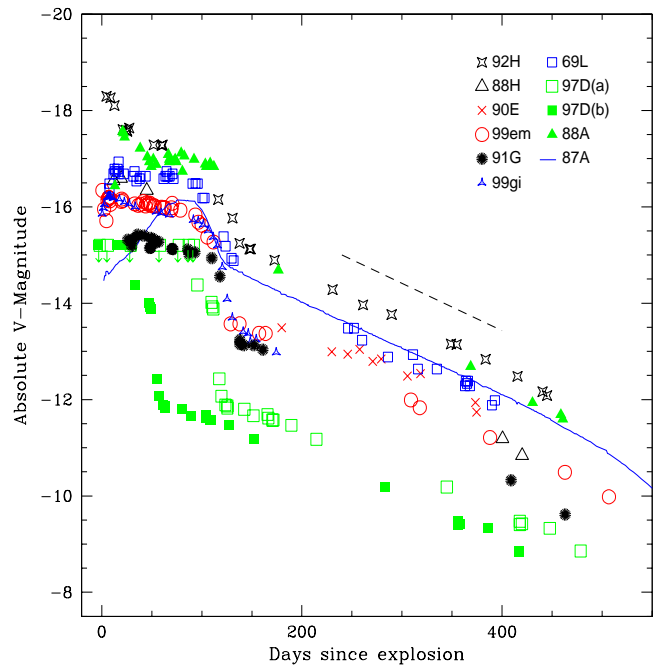
9- Turatto et al. 1993; 10- Blanton et al. 1995; 11- Benetti et al. 1994; 12- Turatto et al. 1998;

13- Benetti et al. 2001; 14- Schmidt et al. 1993; 15- Clocchiatti et al. 1996; 16- Zampieri et al. 2002

17- Barbon et al. 1973; 18- Leonard et al. 2002; 19- Pastorello et al. 2003

* $H_0=70 \text{ km s}^{-1}\text{Mpc}^{-1}$ is adopted.

The recovered total visual reddening (A_V^{tot}) of our sample is listed in Table 1. Fig. 1, on the other hand, displays the intrinsic $B - V$ and $V - R$ colour evolution. Note that for the case of SN 1997D, both colours show a large excess by the end of the photospheric phase. The small (case b; Turatto et al. 1998) and large (case a; Zampieri et al. 2002) age scenarios are displayed. This high reddening seems unlikely since the presence of interstellar lines was not reported in the early spectra as one may expect in a case with such high reddening (Turatto et al. 1998). The very red colour at the end of the photospheric phase is seen in other objects with a very low ejected ^{56}Ni mass (e.g. SN 1999eu; Pastorello et al. 2003, in preparation). An explanation of this peculiarity may be related to the fast cooling from the plateau phase to reach the faint radioactive tail, and/or possibly relates to the nature and structure of the progenitor star. Interestingly, the late nebular intrinsic $B - V$ colours of the complete sample seem to be very similar to that of SN 1987A, both in slope and magnitude. The convergence to the same fate at later phases is also confirmed for the faint object SN 1997D and as well as for the underluminous SN 1999eu (Pastorello et al. 2003). Although studying the spectral energy distribution (SED) of SNe IIP is beyond the scope of the present work, the fact of a small scatter ($\sim \pm 0.3 \text{ mag}$) in the sample around the SN 1987A intrinsic $(B - V)_0$ colour indicates the similarity in the SED for SNe IIP on the radioactive tail. The distance of $D = 50 \text{ kpc}$ is used for SN 1987A, while for the other SNe we adopt distances derived from the recession velocity of the host galaxy corrected for Local Group infall onto the Virgo Cluster as reported in the ‘‘LEDA¹’’ extragalactic

**Fig. 2.** The absolute V -magnitude evolution of the SNe sample. The used parameters are reported in Table 1. Both possibilities for SN 1997D are plotted. The dashed line shows the slope for ^{56}Co decay.

database. The Hubble constant $H_0=70 \text{ km s}^{-1}\text{Mpc}^{-1}$ is adopted. The computed distances are reported in third column of Table 1. We note here that a possibly more accurate value of the distance to SN 1999em, 7.8 Mpc,

¹ available online at <http://leda.univ-lyon1.fr/cgi-bin/single.pl>

Table 2. ^{56}Ni mass estimates from photometry

SN name	$M_{\text{Ni}}(V)$ (M_{\odot})	t_i (days)
1987A	0.075	107 (± 2)
1969L	0.067 (± 0.002)	110 (± 4)
1988A	0.088 (± 0.003)	134 (± 4)
1988H	0.033 (± 0.004)	---
1990E	0.043 (± 0.0024)	---
1991G	0.021 (± 0.0032)	122 (± 5)
1992H	0.123 (± 0.002)	112 (± 5)
1997D(a)	0.0065 (± 0.0003)	112 (± 5)
1997D(b)	0.0036 (± 0.0002)	112 (± 5)
1999em	0.027 (± 0.002)	112 (± 4)
1970G	0.051 (± 0.003)	94 (± 4)
1999gi	0.0246 (± 0.0007)	120 (± 3)
1999eu	0.0028*	110 (± 4)

* From Pastorello et al. 2003 (In preparation)

comes from stellar studies of the parent galaxy NGC 1637 (Sohn & Davidge 1998).

3. ^{56}Ni mass from V light curve

The luminosity of SN IIP on the radioactive tail is controlled by the radioactive decay ($^{56}\text{Co} \rightarrow ^{56}\text{Fe}$) and if the trapping of gamma rays is efficient, the decline rates of the light curves of SNe II should converge to the exponential life-time of ^{56}Co (i.e. 111.26 days or 0.976 mag per 100 d). The radioactive tails in SN IIP all show similar decay rates, especially in the V band (Patat et al. 1994). This fact provides a solid basis for using the V light curve for the recovery of the ejected ^{56}Ni mass (Phillips et al. 1990; Schmidt et al. 1993). In Fig. 2 we display the absolute V light curves of the SNe sample together with that of SN 1987A. The computed late time decline slopes (150 – 400 days since explosion) are reported as well in Table 1 (fifth column). Their mean value is $\langle \gamma^V \rangle \simeq 0.99 (\pm 0.13)$, consistent with the radioactive decay of ^{56}Co and consequent trapping of the gamma-rays.

The ^{56}Ni mass is estimated from absolute M_V magnitudes between 120 – 400 d using the SN 1987A tail as a template. Results produced by the least squares fit are reported in Table 2. Both possible cases for SN 1997D are reported (more details concerning this event are discussed in sect. 4.2). These values show a significant range of the ejected ^{56}Ni masses, from 0.0028 M_{\odot} and 0.0036 M_{\odot} for subluminous SN 1999eu and SN 1997D(case b) respectively to 0.123 M_{\odot} for SN 1992H with the average value $\approx 0.05 M_{\odot}$. Our values differ somewhat from those determined recently by Hamuy (2003) for objects in common. The differences stem primarily from the different distances adopted here. As noted earlier the methodology followed by Hamuy is based upon the conversion of V magnitude into a bolometric luminosity through an assumed constant

bolometric correction, while we are adopting SN 1987A luminosities as a template at late epochs.

With our values of the ^{56}Ni masses it is instructive to check that the correlation between plateau M_V magnitude and the amount of ^{56}Ni found by Hamuy (2003) is preserved. We have modified the definition of the plateau M_V magnitude compared to Hamuy (2003) in order to avoid any uncertainty in the explosion time. Therefore, we use the inflection time during transition from plateau to the radioactive tail as a zero point. The inflection time t_i is defined as the moment when the first derivative at the transition phase $S = -dM_V/dt$ (we dub it “steepness”) is maximal. To calculate S we use the following procedure. The V band flux in the transition period from plateau and radioactive tail is approximated by a sum of plateau and radioactive terms:

$$F = A \frac{(t/t_0)^p}{1 + (t/t_0)^q} + B \exp(-t/111.26), \quad (1)$$

where A , B , t_0 , p and q are parameters derived by the χ^2 minimization technique in the sensitive interval $t_i \pm 50$ days. The behaviour of S and determination of t_i is demonstrated for each SN in Fig. 3. The derived t_i are reported in Table 2 (third column) with the corresponding errors while the computed S values and their errors are presented in Fig. 5. The errors in S and t_i are estimated according to the best fit (shown in Fig. 3) and as well by introducing test points for events with poor data especially at the transition phase (from plateau to radioactive decay). With the determined inflection time t_i we choose the epoch $t_i - 35$ days as a reference for the M_V on the plateau.

Fig. 4 (upper panel) demonstrates the correlation between photometric ^{56}Ni mass and the absolute magnitude $M_V(t_i - 35)$ for the sample of SNe IIP with measurable S and t_i values. This plot shows small scatter around a linear trend and thus supports the correlation found by Hamuy (2003). In our case, and assuming case “a” (Zampieri et al. 2002) for SN 1997D, the linear correlation is described by the equation:

$$\log M(^{56}\text{Ni}) = -0.438 M_V(t_i - 35) - 8.46. \quad (2)$$

Therefore this result suggests a direct correlation between V magnitudes (absolute or apparent) of plateau and radioactive tail. In fact Fig. 4 (lower panel) demonstrates the correlation between M_V magnitudes at plateau (on $t_i - 35$ day) and tail (on $t_i + 35$ day). This is therefore a direct form of the correlation shown in the upper panel.

The sample we explore reveals another interesting correlation. Fig. 5 demonstrates that the steepness S anticorrelates with ^{56}Ni mass: the lower is the ^{56}Ni mass the larger is S , i.e. the steeper is the transition from plateau to the tail. We note however, that an accurate determination of S necessitates a V light curve with a reasonably high density of observational points at the end of the plateau phase and the beginning of the radioactive tail. Indeed SNe 1990E and 1988H are not studied here because of

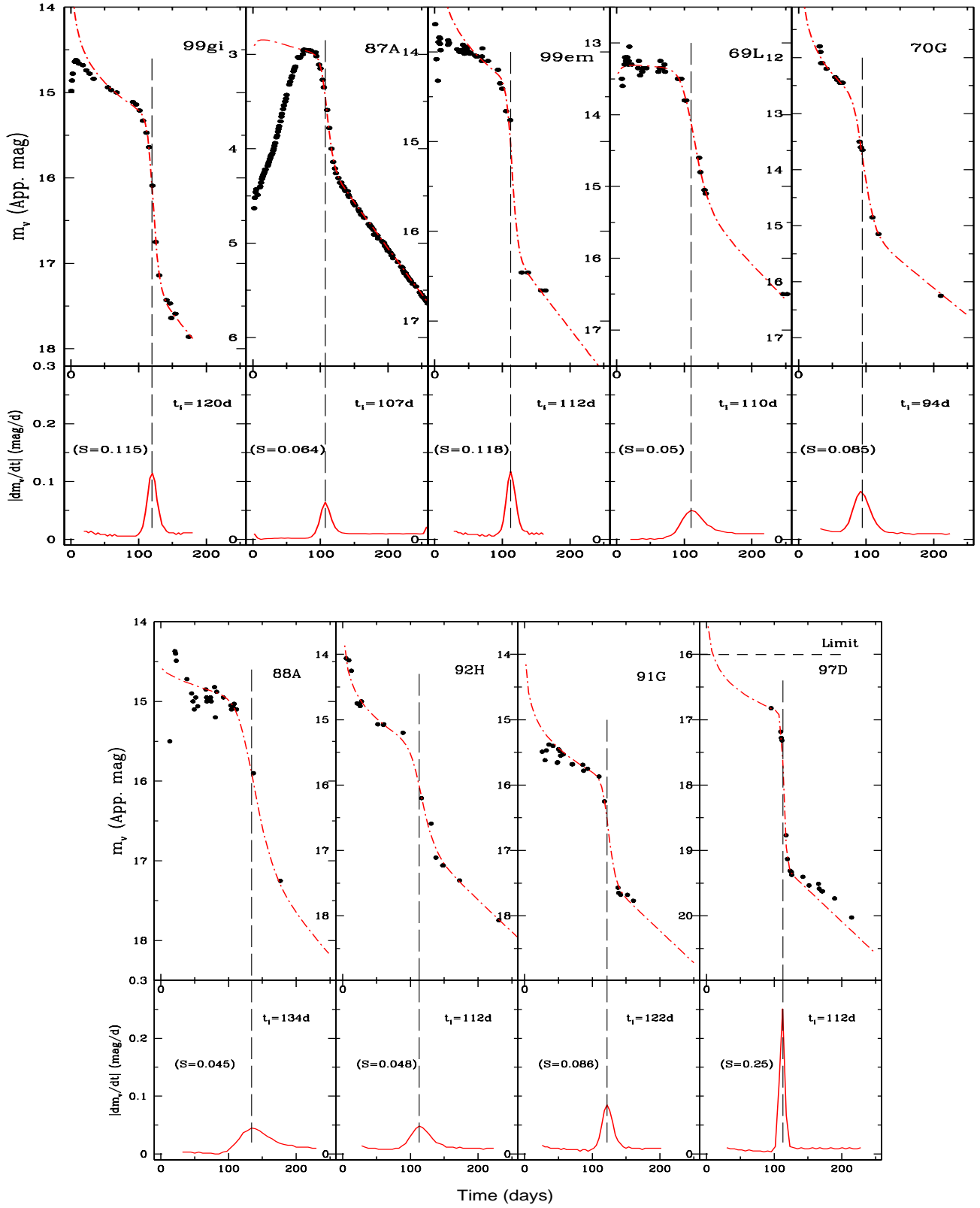


Fig. 3. Determination of the steepness and moment of inflection. For each SN of the sample: upper panel displays the V light curve (dotted points) together with the best fit (dashed curve) while lower panel shows the steepness S (see text). The inflection point t_i shown by dashed line corresponds to the maximum of S . SN 1999eu is not shown because the data is not yet published.

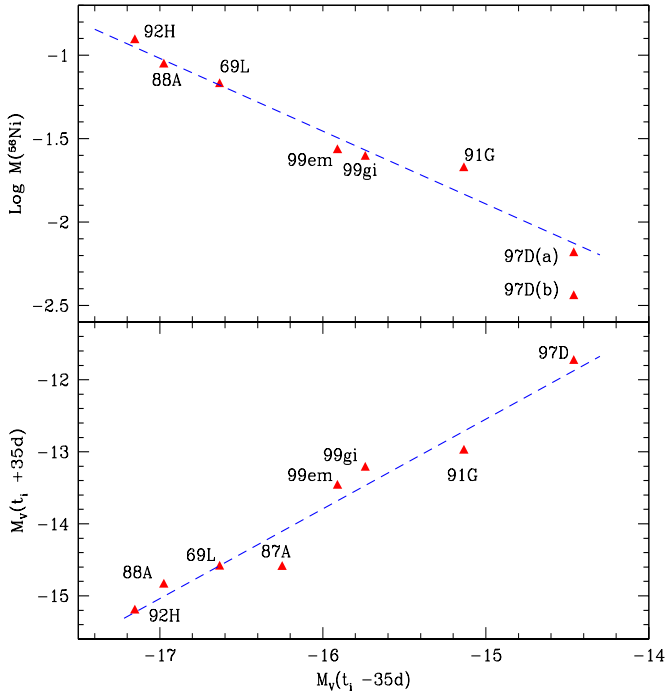


Fig. 4. The correlation between M_V magnitudes of plateau and of radioactive tail. Upper panel shows the correlation between M_V at the moment $(t_i - 35\text{d})$ and ^{56}Ni mass derived from the tail magnitudes; case “a” of SN 1997D is adopted for the fit. Lower panel shows directly the correlation of plateau magnitude $M_V(t_i - 35\text{d})$ and tail magnitude $M_V(t_i + 35\text{d})$.

the paucity of their light curve data. The best linear fit (Fig. 5) reads:

$$\log M(^{56}\text{Ni}) = -6.2295 S - 0.8147 \quad (3)$$

The interpretation of this correlation requires hydrodynamical modeling with different amounts of ^{56}Ni and degrees of mixing. In the case of unmixed ^{56}Ni one does not expect a notable dependence of the steepness on the amount of ^{56}Ni . This is readily seen from the modeling SNe IIP light curves by Eastman et al. (1994). For the same amount of ^{56}Ni the mixing results in a decreased steepness because of an increase of radiative diffusion (Eastman et al. 1994). Unfortunately, in the cited paper the authors did not model cases of variable ^{56}Ni mass with similar degrees of mixing, so the question of the physics behind the above correlation, remains open. At this stage, we may only suggest that somehow the increase of the ^{56}Ni mass in SNe IIP ejecta favours the larger contribution of radiative diffusion at the end of the plateau and, therefore, a less steep transition from plateau to the radioactive tail. It may well be that the increase of the ^{56}Ni mass is accompanied by the growth of the degree of mixing degree which favours a less steep decline as demonstrated in Fig. 10 and Fig. 12 of Eastman et al. (1994).

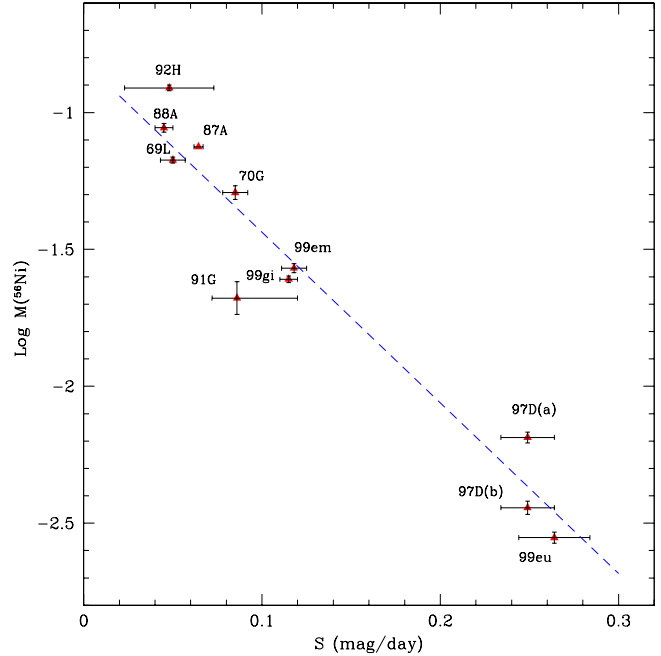


Fig. 5. The correlation between ^{56}Ni mass and steepness S . Case “a” of SN 1997D is adopted for the linear fit (dashed line).

Interestingly, if the correlation between steepness and ^{56}Ni mass is confirmed, this will provide us with an exciting possibility of probing ^{56}Ni mass in SNe IIP from the light curve shape in a manner independent of the distance and extinction.

4. ^{56}Ni mass from $\text{H}\alpha$ luminosity

The $\text{H}\alpha$ luminosity of SNe IIP at late epochs reflects the total ionization in the weakly ionized gas caused by radioactive decay of ^{56}Co and, therefore, to a first approximation is proportional to the overall deposition rate and hence to the ^{56}Ni mass (Chugai 1990; Xu et al. 1992; Kozma & Fransson 1992) unless effects due to higher densities become important. This suggests that the $\text{H}\alpha$ luminosity resulting from gamma-ray trapping may provide a quantitative measure of the ^{56}Ni mass in SNe IIP. The accurate measurements on SN 1987A provide a control. To explore deviations from the simple proportionality we use an upgraded radioactive model of the $\text{H}\alpha$ luminosity.

4.1. Model of $\text{H}\alpha$ luminosity

Some brief comments about the modified model of $\text{H}\alpha$ luminosity powered by the radioactive decay are in order. The primary purpose of the modification of the previous version (Chugai 1990) is to specify better the early nebular phase. This was done by the implementation of macroscopic mixing, collisional and radiative de-excitation effects. The supernova envelope is mimicked by two zones.

Table 3. Parameters of the $\text{H}\alpha$ evolutionary models

Parameter	Unit	Standard	a	a1	b	b1	b2	c	d	e	f	f1
M	M_{\odot}	14	10	7	14	14	14	14	14	14	14	14
E	10^{51}	1	1	1	1	1	1	1.5	1	1	1	1
M_{Ni}	M_{\odot}	0.075	0.075	0.075	0.0375	0.00375	0.15	0.075	0.075	0.075	0.075	0.075
f_{mix}		0.4	0.4	0.4	0.4	0.4	0.4	0.4	0.4	0.1	0.4	0.4
f_{met}		0.2	0.2	0.2	0.2	0.2	0.2	0.2	0.2	0.2	0.3	0.6
T_c	K	7000	7000	7000	7000	7000	7000	7000	5000	7000	7000	7000

The inner zone with the radius $r_{\text{mix}} = v_{\text{mix}}t$ is a mixing core with a total mass fraction f_{mix} , which is divided between metals together with He-rich matter (we dub this mixture “metals” with the mass fraction of f_m) and H-rich matter with the mass fraction $1 - f_{\text{mix}}$. The outer zone consists of hydrogen-rich matter. All the ^{56}Ni resides in the mixing core and has a generally clumpy distribution. This is mimicked by ^{56}Ni clumps in cocoons of metals with the total area of cocoons being $4\pi r_{\text{mix}}^2 f_s$. Here f_s is a mixing parameter, which is unity if all metals reside in the spherical layer with the inner spherical cavity occupied by ^{56}Ni . We adopt $f_s = 2$ which corresponds to moderate mixing. The escape probability for gamma-rays through the metal layer is $\exp(-\tau_m)$, where τ_m is the optical depth of the metal layer, while the absorption probability in the mixing zone is described by the expression $\tau_1/(1 + \tau_1)$, where τ_1 is the optical depth of the inner zone. In the mixing core gamma-rays have a finite probability of being absorbed by H-rich material, which is proportional to $1 - f_{\text{mix}}$. The absorption probability for the outer hydrogen layer with the optical depth τ_2 is defined as $p_2 = 1 - \exp(-\tau_2)$.

The energy deposited in the hydrogen is shared between ionization, excitation and thermal energy with corresponding branching ratios (Kozma & Fransson 1992; Xu et al. 1992). The ionization of hydrogen is calculated in the approximation of three levels plus continuum. The photoionization from the second level by two-photon and continuum radiation was calculated assuming the continuum luminosity is equal to the deposited luminosity while the spectrum is assumed to be dilute black-body with the temperature T_c . The electron temperature was set to be 5000 K. Effects of radiation transfer in Balmer and Paschen continua are treated in the escape probability approximation (Chugai 1990).

The sensitivity of the radioactive model to parameter variations (Table 3) is demonstrated in Fig. 6. Each panel shows the effect of a single parameter variation compared to a standard model, which is in fact the optimal model for the $\text{H}\alpha$ luminosity of SN 1987A. The saturation at the early epoch is a new feature compared to the previous model and this is related to several factors: gamma-ray trapping in the inner zone, collisional de-excitation of the third level and $\text{H}\alpha$ absorption in the Paschen continuum, especially in the mixing zone. In Fig. 6a we present models with lower mass (10 and 7 M_{\odot}) compared to the standard

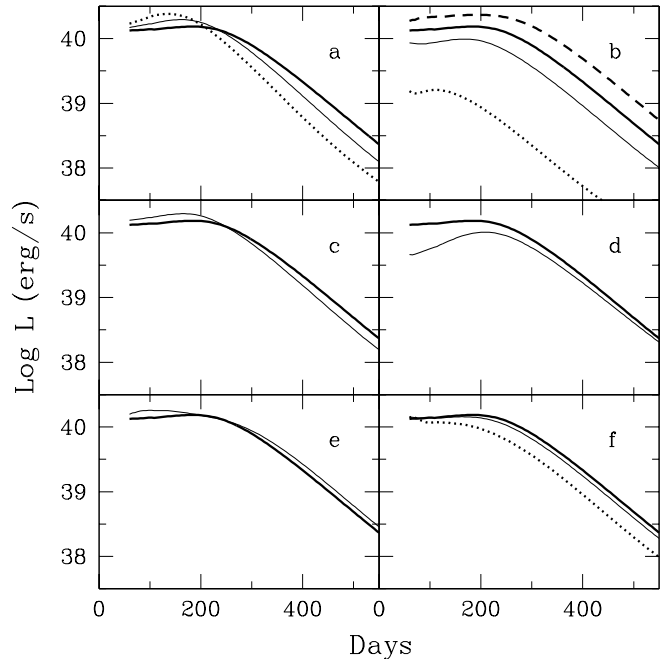


Fig. 6. The $\text{H}\alpha$ luminosity in the radioactive model. The *thick line* shows the standard model, while *thin line* curves show models *a*, *b*, *c*, *d*, *e*, *f*. Dotted lines in panels *a*, *b* and *f* correspond to models *a1*, *b1* and *f1* respectively. Additional model is shown in panel *b* (model *b2*, *dashed line*). Details of model parameters are presented in Table 3.

14 M_{\odot} . A lower mass results in a high rate of the luminosity decay owing to a lower optical depth for gamma-rays. For moderate mass variation (factor ≤ 1.4) the $\text{H}\alpha$ luminosity in the range 200 – 300 d shows less than 10% deviation from the standard case. With the rest of parameters fixed the $\text{H}\alpha$ luminosity is proportional to the ^{56}Ni mass (Fig. 6b) at the nebular epoch $t > 200$ days. This property reflects the simple truth that to a good approximation the total ionization rate of hydrogen in the envelope is proportional to the total radioactive decay rate, i.e. ^{56}Ni mass. The proportionality, however, breaks down for $t < 200$ days because of saturation effects related to $\text{H}\alpha$ collisional de-excitation and continuum absorption, which

become important at early epoch. The effect of factor 1.5 higher kinetic energy is similar to the effect of factor ~ 1.2 lower mass (Fig. 6c), in accordance with the dependence of optical depth on both parameters $\tau_\gamma \propto M^2/E$. A lower continuum temperature (Fig. 6d) results in a lower luminosity, especially, at the early epoch ($t < 200$ d) since the ionization (and therefore recombination) rate becomes lower. A lower mixing core fraction (Fig. 6e) results in the higher $\text{H}\alpha$ luminosity since the total deposition in the outer H-rich matter increases. The higher metal fraction in the mixing core (Fig. 6f), on the contrary, suppresses the late time $\text{H}\alpha$ luminosity consistent with the decreased deposition into mixed hydrogen material. However, this effect is small if the variation of this parameter is within a factor 1.5.

The modeling shows that if ejecta parameters vary less than a factor 1.4 compared to those of SN 1987A, the $\text{H}\alpha$ luminosity is then proportional to the ^{56}Ni mass (to within 10% accuracy) at the late time nebular phase 200 – 400 days. In this age range using the SN 1987A model as a template we may estimate the ^{56}Ni mass in other SNe IIP from the ratio of $\text{H}\alpha$ luminosity to that of SN 1987A. It is worth noting here that despite the large possible variation of the main sequence mass for SNe IIP, presumably say 10 – 25 M_\odot , the range in mass of the ejecta may actually be smaller since mass loss increases rapidly with the mass.

4.2. Results of ^{56}Ni mass determination

The spectra utilized in this section are based on data in the Asiago/ESO SN Catalogue. Additional spectra were kindly provided by R. Stathakis. A sample of the spectra is shown in Fig. 7 together with some line identifications. The available spectra of our sample were corrected for reddening effects and the recovered integrated $\text{H}\alpha$ line fluxes are then translated to luminosities using adopted distances. In a straightforward approach we use the $\text{H}\alpha$ luminosity of SN 1987A as a template to recover the ^{56}Ni mass from the $\text{H}\alpha$ luminosity of SNe IIP assuming proportionality between the ^{56}Ni mass and the $\text{H}\alpha$ luminosity in the range between 200 – 400 days. The resulting values of ^{56}Ni mass are given in Table 4 in the second column.

Another approach has been to fit the $\text{H}\alpha$ light curves with the model of luminosity evolution. All the other parameters, except for ^{56}Ni mass, are assumed to be the same as in the standard model for SN 1987A unless additional information indicates essentially different parameters. The plateau of SN 1970G is very brief ($t_p \approx 60$ d) which indicates a lower ejecta mass than that of a typical SN IIP. We adopt 8 M_\odot as the most appropriate value for SN 1970G ejecta taking into account both the light curve and the rate of the $\text{H}\alpha$ flux decay. The results are plotted for 9 SNe in Fig. 8. Recovered values of ^{56}Ni mass are given in Table 4 (third column). Note that the straightforward approach based upon the use of the $\text{H}\alpha$ light curve of SN 1987A (second column of Table 4) and the application of model fitting produce quite similar values with

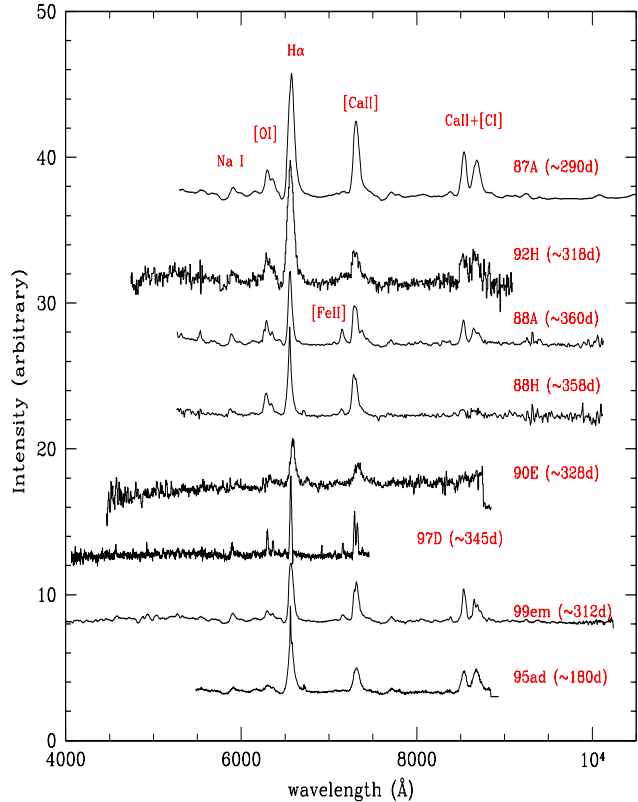


Fig. 7. Sample of late time spectra of SNe IIP with the corresponding time since explosion. The spectra have been corrected for the recession velocities of their host galaxies. Some line identifications are also indicated.

a maximal difference, apart from SN 1970G(SNP/L) and SN 1997D(treated below), of $\sim 13\%$ for SN 1988H.

This deviation may be adopted as an uncertainty of the ^{56}Ni mass determination from the accurate data. Given the uncertainty of the observed value of the $\text{H}\alpha$ luminosity (at least 10%) we are therefore able to derive a ^{56}Ni mass from $\text{H}\alpha$ with an uncertainty of about 25%.

The subluminous SN 1997D is a special case. Originally, the age of the supernova at discovery has been estimated to be $t_d = 50$ days (Turatto et al. 1998), while Zampieri et al. (2002) argue for an age almost twice as large $t_d \approx 95$ days. We consider both large and small age options. In the large age case we adopt $M = 18 M_\odot$, $E = 9 \times 10^{50}$ erg (Zampieri et al. 2002), while in the small age option we adopt $M = 6 M_\odot$ and $E = 1 \times 10^{50}$ erg (Chugai & Utrobin 2000). A reasonable fit in the first case (Fig. 9a) is found for the ^{56}Ni mass of 0.011 M_\odot with a mixed core fraction $f_{\text{mix}} = 0.05$, which corresponds to the mixing core having 0.9 M_\odot and a core metal fraction $f_m = 0.99$, i.e. with the metal core practically devoid of hydrogen. The model also requires a low continuum temperature in the ultraviolet $T_c = 4500$ K. For the small age choice the fit (Fig. 9b) corresponds to $M(^{56}\text{Ni}) = 0.0024 M_\odot$. In this case $f_{\text{mix}} = 0.05$,

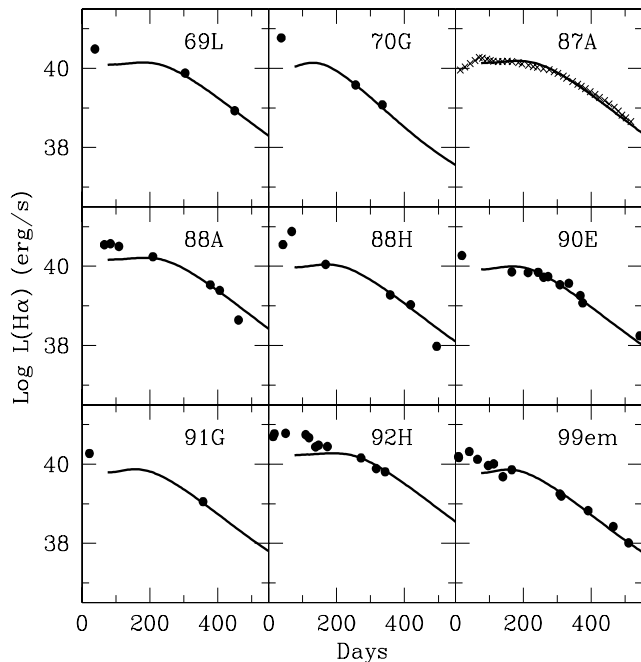


Fig. 8. The $\text{H}\alpha$ luminosity evolution in different SN IIP. Models (*solid lines*) are overlotted on the observational data *dots* (sect. 4.2).

$f_m = 0.3$ (a significant amount of mixed hydrogen) and $T_c = 5500$ K.

The ^{56}Ni mass derived from the $\text{H}\alpha$ luminosity adopting SN 1987A as template, $M_{\text{Ni}}(\text{H}\alpha)$, is plotted in Fig. 10 versus photometric ^{56}Ni mass, $M_{\text{Ni}}(V)$, derived from the tail M_V magnitude (Table 2). Both sets of values agree within 20%. This consistency supports the proposition that the $\text{H}\alpha$ luminosity may be a good indicator of ^{56}Ni mass in SNe IIP unless we are dealing with extreme cases such as SN 1970G (SNP/L) or underluminous cases such as SN 1997D.

4.3. Application of $\text{H}\alpha$ to ^{56}Ni diagnostics

In the absence of the late time photometry but with available spectra of SNe IIP at the nebular epoch we may use the $\text{H}\alpha$ luminosity to estimate ^{56}Ni mass ejected by supernova provided the explosion time is known. We demonstrate this approach to SN 1995ad, SN 1995V and SN 1995W (all type IIP) for which late photometric data are not available. Distances are computed using the corrected recession velocities (reported in “LEDA” data base assuming $H_0 = 70 \text{ km s}^{-1} \text{ Mpc}^{-1}$).

SN 1995ad: This SN was discovered on Sep. 28.8 UT in NGC 2139 by R. Evans (IAUC 6239). Its Sep. 29.3 UT spectrum, obtained by S. Benetti, displays a hot continuum with temperature $T_{bb} \sim 13000$ K and a broad $\text{H}\alpha$ emission ($FWHM = 11000 \text{ km s}^{-1}$). These characteristics combined with the fact that nothing was seen at the

Table 4. Recovered mass of ^{56}Ni using SN 1987A as template (second column), and from late time L($\text{H}\alpha$) modeling “ $M_{\text{Ni}}^m(\text{H}\alpha)$ ”.

SN name	$M_{\text{Ni}}(\text{H}\alpha)$ (M_\odot)	$M_{\text{Ni}}^m(\text{H}\alpha)$ (M_\odot)
1969L	0.068(± 0.004)	0.065
1970G	0.029(± 0.011)	0.035
1988A	0.085(± 0.004)	0.083
1988H	0.039(± 0.005)	0.045
1990E	0.04(± 0.003)	0.038
1991G	0.022(± 0.0005)	0.025
1992H	0.106(± 0.008)	0.105
1997D(a)	0.0028(± 0.0006)	0.011
1997D(b)	0.0018(± 0.0004)	0.0024
1999em	0.022(± 0.003)	0.024

position of the SN in the Aug. 25 image (IAUC 6239) provide constraints on the explosion time. The assumed distance and reddening are respectively $D = 23.52$ Mpc and $A_V = 0.112$ mag (NED; Schlegel et al. 1998) while the galaxy inclination is 40.9° . The spectrum we use here is taken 1996 March. 24, about 180 days since explosion. The derived $\text{H}\alpha$ luminosity, $\sim 1.06 \times 10^{40} \text{ erg s}^{-1}$, is then compared to that of SN 1987A at a similar epoch to recover an ejected mass $\approx 0.056 \odot M_\odot$.

SN 1995V: discovered in NGC 1087 by R. Evans (IAUC 6197). The galaxy inclination is 33.2° . The adopted distance and reddening are, accordingly, $D = 20.61$ Mpc and $A_V = 1.37$ mag, while the explosion time is assumed to be 1995 July. 25 (Fassia et al. 1998). The available late spectrum was taken around day 409 since explosion. Comparing the recovered $\text{H}\alpha$ luminosity, $\sim 1.33 \times 10^{39} \text{ erg s}^{-1}$, with that of SN 1987A leads to the estimate of $M(^{56}\text{Ni}) \approx 0.046 M_\odot$.

SN 1995W: discovered on Aug. 5.65 UT in NGC 7650 by A. Williams and R. Martin (IAUC 6206). The spectrum taken on Aug 17.29 UT displayed features of SN IIP around one month (IAUC 6206). The distance is $D = 44.81$ Mpc, and the reddening is $A_V = 0.044$ mag (NED; Schlegel et al. 1998) and the host galaxy inclination is 47.4° . The late spectrum was taken around day 300 (1996 May. 12). The $\text{H}\alpha$ luminosity, $\sim 4.79 \times 10^{39} \text{ erg s}^{-1}$, when compared to that of SN 1987A at similar epoch yields an amount of ^{56}Ni mass of $M(^{56}\text{Ni}) \approx 0.048 M_\odot$. Note that the adopted reddening values for SN 1995ad and SN 1995W do not include the host galaxy reddening. For these events the inclination of their host galaxies may provide further indication of uncertainty in the extinction since large extinctions might be expected for highly inclined galaxies if the SN occurred towards the far side. Although no sign of high extinction from interstellar lines was reported in early spectra of these two objects, the derived amounts of $M(^{56}\text{Ni})$ might be taken as lower limits bearing in mind the significant inclination of their host galaxies.

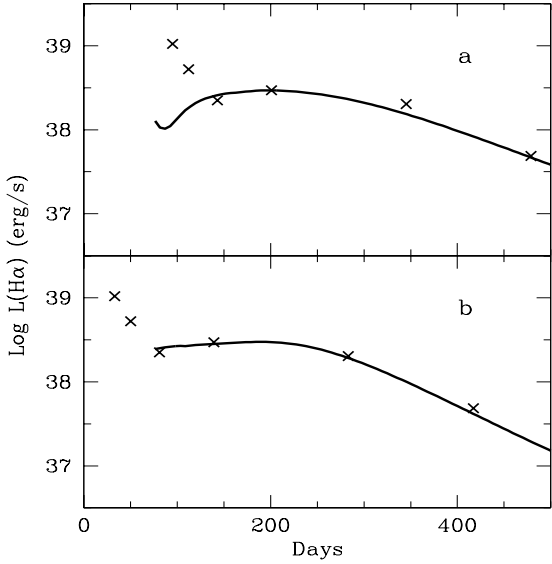


Fig. 9. Modeling $\text{H}\alpha$ luminosity for SN 1997D. The upper panel shows the large age option, while lower panel shows the small age option. Model results (*solid lines*) are overplotted on observational dots.

5. Discussion and conclusion

The primary goal of this paper was to demonstrate that the $\text{H}\alpha$ luminosity at the nebular epoch may be an indicator of the ^{56}Ni mass in SNe IIP ejecta. To explore this idea we selected a sample of well observed SNe IIP, and using V magnitudes on the radioactive tail we derived in a standard way the photometric mass of ^{56}Ni mass. With our sample we confirmed using a slightly different approach the correlation between ^{56}Ni mass and absolute magnitude M_V of the plateau reported recently by Hamuy (2003). We then applied a two-zone model of the $\text{H}\alpha$ luminosity in SN IIP to explore the sensitivity of the $\text{H}\alpha$ behaviour to variation of model parameters. We found that if mass, energy and mixing conditions do not vary strongly among SNe IIP (less than factor 1.4) then with an accuracy better than 10% $\text{H}\alpha$ luminosity is proportional to ^{56}Ni mass during the 200 – 400 days after explosion. $\text{H}\alpha$ luminosities were then used to derive ^{56}Ni masses. This was done employing two approaches: first, using the $\text{H}\alpha$ light curve in SN 1987A as template and, second, applying the model computations. Both approaches agree within 15% unless we are dealing with extreme cases such as SN 1970G (type IIP/L) and underluminous SN 1997D. In both these cases we should possess additional information about ejecta mass and energy to derive the ^{56}Ni mass from $\text{H}\alpha$. The ^{56}Ni mass values derived from the photometry and $\text{H}\alpha$ luminosity agree within 20%, which thus gives us confidence that $\text{H}\alpha$ is a good indicator of the amount of ^{56}Ni in SNe IIP. Simultaneously, this consistency suggests that parameters of SNe IIP (mass, energy and mixing) are not very different. In fact this is consistent with the

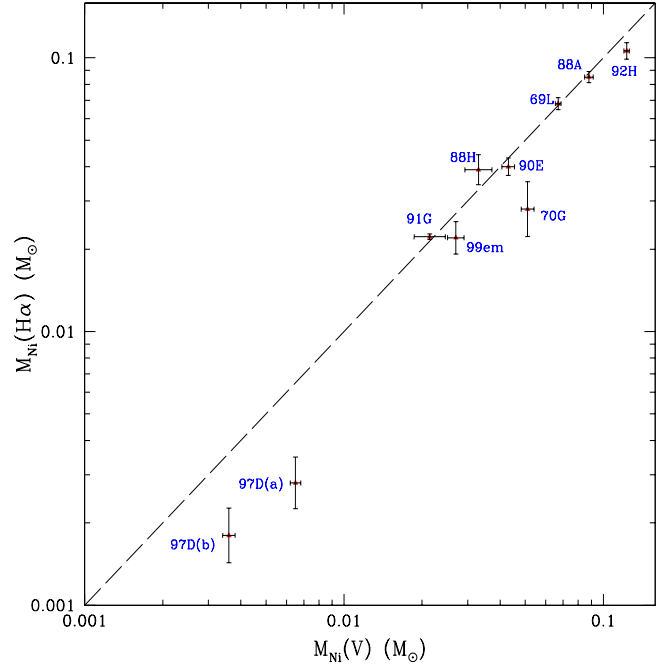


Fig. 10. The correlation between the ^{56}Ni mass derived from the $\text{H}\alpha$ luminosity, $M_{\text{Ni}}(\text{H}\alpha)$, and that derived from the tail M_V magnitude, $M_{\text{Ni}}(V)$. The dashed line has a slope of unity. Clear deviation is seen for SN 1970G(SNP/L) and for both scenarios of the faint event SN 1997D.

uniformity of plateau luminosities and plateau lengths of SNe IIP.

We applied the method of ^{56}Ni mass estimation from $\text{H}\alpha$ for three SNe IIP (SN 1995ad, SN 1995V and SN 1995W) without photometry at the nebular phase and derived ^{56}Ni masses of $\approx 0.056 M_{\odot}$, $0.046 M_{\odot}$, $0.048 M_{\odot}$, quite reasonable values, although they could be underestimates, since the host galaxy extinction (for SN 1995ad & 1995W) has not been taken into account. Nevertheless, this is a good demonstration of the possibility of the method. Generally, the approach based upon $\text{H}\alpha$ may be indispensable in cases, when the photometry at the nebular epoch is absent, or when there is a problem with subtraction of stellar background (SN IIP in the bulge, or in high redshift galaxies).

An interesting by-product of the analysis of the SNe IIP sample is the demonstrated correlation between ^{56}Ni mass and the steepness parameter (S) introduced to measure the light curve decay rate at the inflection point. The correlation is such that the steeper the decline at the inflection point the lower is the ^{56}Ni mass. Thus radiative diffusion times and ^{56}Ni masses are linked. How an increased radioactive energy input leads to a higher effective opacity will require elaboration by hydrodynamical modeling. This correlation, if confirmed, will provide us with a distance and extinction independent way to determine the amount of ejected ^{56}Ni .

Finally we note that in Fig. 10 the clustering of the points around two values of ^{56}Ni mass viz. 0.005 and 0.05 M_{\odot} may result from poor statistical sampling. On the other hand it may be a hint that a mechanism such as fall-back is an important one in the evolution of the low-mass group.

Acknowledgements. We thank Raylee Stathakis for providing us with some unpublished spectra in the AAO Archive which were useful for measurements of $\text{H}\alpha$ luminosities. A. Elmhamdi thanks A. Pastorello for providing some data for SN 1999eu. Research by N. N. Chugai was supported by grant “RFBR 01-02-16295” of Russian Academy of Sciences.

References

- Arnett W. D. 1996, in “Supernovae and nucleosynthesis”, (Princeton University Press)
- Aufderheide M. B., Baron E. & Thielemann F. K. 1991, *ApJ*, 370, 630
- Barbon R., Ciatti F. & Rosino L. 1973, *A&A*, 29, 57
- Baron E., Branch D, Hauschildt P. et al. 2000, *ApJ*, 545, 444
- Benetti S., Cappellaro E., Turatto M. et al. 1994, *A&A*, 285, 147
- Benetti S., Turatto M., Balberg S. et al. 2001, *MNRAS* 322, 361
- Bouchet P. & Danziger I. J. 1993, *A&A*, 273, 451
- Blanton E. L., Schmidt B. P., Kirshner R. P. et al. 1995, *AJ*, 110, 2868
- Cardelli J. A., Clayton G. C. & Mathis J. S. 1989, *ApJ*, 345, 245
- Catchpole R. M., Whitelock P. A., Feast M. W. et al. 1988, *MNRAS*, 231, 75
- Chugai N. N. 1990, *SvAL*, 16, 457
- Chugai N. N. & Utrobin V. P. 2000, *A&A*, 354, 557
- Clocchiatti A., Benetti S., Wheeler J. C. et al. 1996, *AJ*, 111, 1286
- Eastman R. G. et al. 1994, *ApJ*, 430, 300
- Elmhamdi A., Danziger I. J., Chugai N. N. et al. 2003, *MNRAS*, 338, 939
- Evans R. O., Jarman J., Cragg T. et al. 1995, *IAUC* 6197
- Evans R., Benetti S. & Grupe D. 1995, *IAUC* 6239
- Fassia A., Meikle W. P. S. Geballe T. R. et al. 1998, *MNRAS*, 299, 150
- Filippenko A. V. 2001, in “Young Supernova Remnants”, ed. S. S. Holt (New York: American Institute of Physics)
- Grassberg E. K., Imshennik V. S. and Nadyozhin D. K. 1971, *Astrophys. Space Sci*, 10, 28
- Hamuy M., Pinto P. A., Maza J. et al. 2001, *ApJ*, 558, 615
- Hamuy M. 2003, *ApJ*, 582, 905
- Hirata K., Kajita T., Koshihara M. et al. 1987, *Phys. Rev. Lett.* 58, 1490
- Kirshner R. P. & Kwan J. 1975, *ApJ*, 197, 412
- Kozma C. & Fransson C. 1992, *ApJ*, 390, 602
- Leonard D. C., Filippenko A. V., Li W. et al. 2002, *AJ*, 124, 2490
- Litvinova I. Y & Nadyozhin D. K. 1985, *SvAL*, 11, 145
- Patat F., Barbon R., Cappellaro E. & Turatto M. 1994, *A&A*, 282, 731
- Phillips M. M., Hamuy M., Maza J. et al. 1990, *PASP*, 102, 299
- Ruiz-Lapuente P., Canal R., Kidger M., Lopez R. et al. 1990, *ApJ*, 100, 782
- Schlegel D. J., Finkbeiner D. P. & Davis M. 1998, 500, 525
- Schmidt B. P., Kirshner R. P. & Eastman R. G. 1992, *ApJ*, 395, 366
- Schmidt B. P., Kirshner R. P., Schild R. et al. 1993, *ApJ*, 105, 2236
- Sohn Y. J. & Davidge T. J. 1998, *AJ*, 115, 143
- Turatto M., Cappellaro E., Benetti S. & Danziger I. J. 1993, *MNRAS*, 265, 471
- Turatto M., Mazzali P. A., Young T. R. et al. 1998, *AJ*, 498, L129-L133
- Weaver T. A. & Woosley S. E. 1980, *Ann. N.Y. Acad. Sci*, 336, 335
- Williams A., Martin R., Greenhill J. et al. 1995, *IAUC* 6206
- Xu Y., McCray R., Oliva E. & Randich S. 1992, *ApJ*, 386, 181
- Zampieri L. et al. 2002, *MNRAS*; in press